$W_2Cl_4(NHR)_2(PR'_3)_2$ Molecules. 3. Bidentate Phosphine Complexes of Bis(*tert*-butylamido)tetrachloroditungsten. Preparation and Structural Characterization of *cis,cis*-$W_2Cl_4(NHCMe_3)_2$(L-L) (L-L = dmpm, dmpe, dppm, dppe)

F. Albert Cotton,* Evgeny V. Dikarev, and Wai-Yeung Wong

Department of Chemistry and Laboratory for Molecular Structure and Bonding, Texas A&M University, College Station, Texas 77843-3255

Received August 1, 1996[⊗]

Four new triply-bonded ditungsten complexes of the formula *cis,cis*-$W_2Cl_4(NHCMe_3)_2$(L-L) (L-L = dmpm (**1**), dmpe (**2**), dppm (**3**), dppe (**4**)) have been prepared by reaction of $W_2Cl_4(NHCMe_3)_2(NH_2CMe_3)_2$ with the appropriate bidentate phosphines (L-L) in hydrocarbon solvents. These complexes are the first triply-bonded complexes of the form $W_2Cl_4(NHR)_2$(L-L) where L-L groups are bidentate phosphines. The molecular structures have been investigated by X-ray crystallography. Crystal data are as follows: for **1**, monoclinic space group $P2_1/n$, a = 13.807(1) Å, b = 11.835(2) Å, c = 15.348(1) Å, β = 109.19(2)°, Z = 4; for **2**, $P2_1/n$, a = 14.144(2) Å, b = 11.991(1) Å, c = 15.662(2) Å, β = 109.50(1)°, Z = 4; for **3**·CH_2Cl_2, $P2_1/c$, a = 18.777(6) Å, b = 10.273(2) Å, c = 21.082(3) Å, β = 94.11(6)°, Z = 4; for **4**, $P2_1/n$, a = 11.938(1) Å, b = 18.583(3) Å, c = 17.606(2) Å, β = 106.54(6)°, Z = 4. The W−W bond lengths for **1**, **2**, **3**·CH_2Cl_2, and **4** are 2.3247(4), 2.3274(5), 2.328(1), and 2.3452(5) Å, respectively, which are consistent with a formal W≡W bond. The W−P and W−Cl distances are similar in all of the complexes reported. The average W−N distance of 1.905(7) Å is indicative of a W−N double bond having some N → W π character. No orientational disorder of the central ditungsten units was observed. While strong N-H···Cl hydrogen bonding is retained in these diphosphine complexes, each molecule deviates from an eclipsed geometry with torsion angles involving the hydrogen-bonded N and Cl atoms being in the range 12.8−22.0°. It is also noteworthy that all complexes are highly twisted and display exceptionally large torsional angles for the bridging diphosphines across the W≡W bond (**1**, 46.2°; **2**, 59.9°; **3**·CH_2Cl_2, 43.6°; **4**, 56.8°). As far as the stereochemistry of each molecule is concerned, the structure analyses reveal that the final product in each case was the *cis,cis* isomer of $W_2Cl_4(NHCMe_3)_2$(L-L) with the P and N atoms mutually cis on each W atom. In addition to the structural data for these complexes, IR, $^{31}P\{^1H\}$ and ^1H NMR spectroscopy, and mass spectrometry have been used to characterize the complexes.

Introduction

We have reported on the chemistry of the isomeric title compounds $W_2Cl_4(NHCMe_3)_2(PR_3)_2$ with monodentate phosphines in parts 1 and 2.[1] However, no examples of compounds having the formula $W_2Cl_4(NHR)_2$(L-L), where L-L is a bridging bidentate phosphine, are known.[2] Besides, relatively few data are available for W_2^{6+} species with the formula $W_2Cl_x(NR_2)_{6-x}$(L-L) containing bidentate phosphines L-L. To our knowledge, only two complexes of this type have been prepared, viz., $W_2Cl_2(NMe_2)_4$(dmpm) and $W_2Cl_2(NMe_2)_4$(dmpe), but no structural characterization has been carried out.[3] In this paper, we report the first $W_2Cl_4(NHCMe_3)_2$(L-L)-type compounds with bridging diphosphines L-L = dmpm, dmpe, dppm, and dppe. Each of these compounds has been characterized by IR, $^{31}P\{^1H\}$ and ^1H NMR spectroscopy, mass spectrometry, and single-crystal X-ray diffraction studies.

Experimental Section

General Procedures. All manipulations were carried out under an atmosphere of dry argon or dinitrogen using standard Schlenk techniques. Commercial grade solvents were dried and deoxygenated by refluxing over appropriate reagents and freshly distilled under dinitrogen immediately prior to use. *tert*-Butylamine, dppm, and dppe were purchased from Aldrich, Inc., and used as received. WCl_4, dmpm, and dmpe were purchased from Strem Chemicals and used as received. The compound $W_2Cl_4(NHCMe_3)_2(NH_2CMe_3)_2$ was prepared according to the published procedure using Na−Hg as the reducing agent.[4]

Syntheses. (i) *cis,cis*-$W_2Cl_4(NHCMe_3)_2$(dmpm) (1). $W_2Cl_4(NHCMe_3)_2(NH_2CMe_3)_2$ (0.5 g, 0.62 mmol) was dissolved in hexanes (10 mL), and dmpm (1 equiv) was added via syringe with constant stirring. The color of the solution immediately changed from orange to red, and a brown-red precipitate formed in a few minutes. Stirring was continued for 1 h, after which the solvent, liberated *tert*-butylamine, and any excess of dmpm were removed under vacuum. The resulting residue was redissolved in a minimum volume of hot toluene to yield a deep-orange solution after filtration through Celite. When hexanes were carefully layered on this solution, red block-shaped crystals of *cis,cis*-$W_2Cl_4(NHCMe_3)_2$(dmpm) (0.22 g, yield 45%) were obtained after 2 days at room temperature.

IR data (cm^{-1}): 3226 (w), 1402 (w), 1301 (w), 1285 (w), 1261 (s), 1217 (w), 1202 (w), 1171 (w), 1094 (s, br), 1019 (s, br), 941 (m), 898 (vw), 863 (w), 801 (vs), 725 (vw), 707 (vw), 701 (vw).

^1H NMR data (benzene-d_6, 24 °C, δ): 1.01 (s, 18H, CMe_3), 1.21 (virtual triplet, J = 5.6 Hz, 6H, PMe_2), 2.08 (virtual triplet, J = 5.6 Hz, 6H, PMe $_2$), 2.19 (t, J = 11.2 Hz, 2H, PCH_2P), 12.80 (br, 2H, NH).

$^{31}P\{^1H\}$ NMR data (benzene-d_6, 19 °C, δ): 10.29 (s, $^1J_{W-P}$ = 150 Hz, $^2J_{P-P}$ = 84.3 Hz).

FAB/DIP (DIP = direct insertion probe) MS (NBA, *m/z*): 790 ($[M]^+$), 754 ($[M - Cl]^+$).

[⊗] Abstract published in *Advance ACS Abstracts,* December 15, 1996.

(1) (a) Cotton, F. A.; Yao, Z. *J. Cluster Sci.* **1994**, *5*, 11. (b) Chen, H.; Cotton, F. A.; Yao, Z. *Inorg. Chem.* **1994**, *33*, 4255.

(2) Cotton, F. A.; Walton, R. A. *Multiple Bonds between Metal Atoms*, 2nd ed.; Oxford University Press: New York, 1993; see also references therein.

(3) Ahmed, K. J.; Chisholm, M. H.; Folting, K.; Huffman, J. C. *Inorg. Chem.* **1985**, *24*, 4039.

(4) Bradley, D. C.; Errington, R. J.; Hursthouse, M. B.; Short, R. L. *J. Chem. Soc., Dalton Trans.* **1986**, 1305.

S0020-1669(96)00906-8 CCC: $14.00

Table 1. Crystallographic Data for *cis,cis*-$W_2Cl_4(NHCMe_3)_2$(dmpm) (**1**), *cis,cis*-$W_2Cl_4(NHCMe_3)_2$(dmpe) (**2**), *cis,cis*-$W_2Cl_4(NHCMe_3)_2$(dppm)·CH_2Cl_2 (**3**·CH_2Cl_2), and *cis,cis*-$W_2Cl_4(NHCMe_3)_2$(dppe) (**4**)

	1	**2**	**3**	**4**
formula	$W_2Cl_4P_2C_{13}H_{34}N_2$	$W_2Cl_4P_2C_{14}H_{36}N_2$	$W_2Cl_6P_2C_{34}H_{44}N_2$	$W_2Cl_4P_2C_{34}H_{44}N_2$
fw	789.86	803.89	1123.05	1052.15
space group (No.)	$P2_1/n$ (14)	$P2_1/n$ (14)	$P2_1/c$ (14)	$P2_1/n$ (14)
a, Å	13.807(1)	14.144(2)	18.777(6)	11.938(1)
b, Å	11.835(2)	11.991(1)	10.273(2)	18.583(3)
c, Å	15.348(1)	15.662(2)	21.082(3)	17.606(2)
β, deg	109.19(2)	109.50(1)	94.11(6)	106.54(6)
V, Å^3	2368.6(5)	2503.9(5)	4056(2)	3744.1(8)
Z	4	4	4	4
ρ_{calc}, g/cm^3	2.215	2.132	1.839	1.867
μ, mm^{-1}	10.292	21.877	6.168	6.537
radiation (λ, Å)	Mo Kα (0.710 73)	Cu Kα (1.541 84)	Mo Kα (0.710 73)	Mo Kα (0.710 73)
temp, °C	−150	20	−60	-60
transm. factors	0.9953−0.4896	1.0000−0.4952	0.300−0.197	none
R1[a], R2[b] [$I > 2\sigma(I)$]	0.032, 0.083	0.034, 0.088	0.042, 0.091	0.050, 0.117
R1[a], R2[b] (all data)	0.039, 0.088	0.042, 0.095	0.056, 0.098	0.062, 0.127

[a] $R1 = \sum||F_o| - |F_c||/\sum|F_o|$. [b] $wR2 = [\sum[w(F_o^2 - F_c^2)^2]/\sum[w(F_o^2)^2]]^{1/2}$.

(ii) *cis,cis*-$W_2Cl_4(NHCMe_3)_2$(dmpe) (2). The synthesis of compound **2** followed a similar course to that of **1**. Upon adding dmpe, the color of the solution changed from orange to dark-red. After 1 h of stirring, all the volatile components of the mixture were removed under reduced pressure. Initial hexanes extraction (15 mL) of the resulting residue afforded a bright-red solution, which was shown by $^{31}P\{^1H\}$ NMR at room temperature to contain a complicated mixture of products which as yet remains uncharacterized. The residue was then extracted with a minimum volume of toluene (10 mL), and the deep-red solution was allowed to stand at room temperature for a week to afford a first crop of red crystals. A second crop of crystals was obtained by keeping the filtrate in a freezer at −15 °C for 2 days. The overall yield was about 39%.

IR data (cm^{-1}): 3203 (m), 1413 (w), 1367 (m), 1361 (m), 1324 (w), 1300 (vw), 1283 (w), 1261 (w), 1218 (w), 1202 (m), 1170 (vw), 1161 (vw), 1092 (m, br), 1022 (w), 949 (s), 921 (m), 870 (w), 844 (w), 798 (m), 793 (m), 745 (w), 728 (w), 709 (w).

^1H NMR data (CD_2Cl_2, 24 °C, δ): 1.22 (s, 18H, CMe_3), 1.46 (d, J = 8.4 Hz, $P(CH_2)_2P$), 1.56 (br, 6H, PMe_2), 2.11 (d, J = 10.2 Hz, $P(CH_2)_2P$), 2.60 (br, 6H, PMe_2), 12.21(br, 2H, NH).

$^{31}P\{^1H\}$ NMR data ($CDCl_3$, 19 °C, δ): 13.74 (s, $^1J_{W-P}$ = 305 Hz, $^3J_{P-P}$ = 31.4 Hz).

FAB/DIP MS (NBA, *m/z*): 804 ($[M]^+$), 767 ($[M - Cl]^+$), 732 ($[M - 2Cl]^+$), 659 ($[M - 2NHCMe_3]^+$).

(iii) *cis,cis*-$W_2Cl_4(NHCMe_3)_2$(dppm) (3). Dppm (0.24 g, 0.62 mmol) was dissolved in toluene (10 mL) and added via cannula to a solution of $W_2Cl_4(NHCMe_3)_2(NH_2CMe_3)_2$ (0.5 g, 0.62 mmol) in hexanes (10 mL). The color started to turn dark-red, and after about 1 h of stirring, the solvent and other volatile components were removed under vacuum. The residual dark-red solid was redissolved in hot toluene (10 mL) to give a deep-red solution. An initial attempt to grow single crystals by layering hexanes on the toluene extract failed. However, bright-red block-shaped crystals of **3** of good X-ray quality (0.27 g, 42%) were obtained in 2 days by layering hexanes over a CH_2Cl_2 solution of **3** at room temperature.

IR data (cm^{-1}): 3202 (w), 3178 (w), 3039 (w), 1485 (m), 1434 (s), 1365 (ms), 1324 (w), 1310 (vw), 1281 (w), 1261 (m), 1200 (s), 1171 (w), 1156 (w), 1146 (w), 1091 (s), 1025 (m), 954 (w), 916 (w), 802 (ms), 791 (ms), 741 (ms), 728 (ms), 694 (s).

^1H NMR data (CD_2Cl_2, 24 °C, δ): 1.18 (s, 18H, CMe $_3$), 5.01 (t, J = 10.6 Hz, 2H, PCH_2P), 7.09−8.03 (m, 20H, Ph), 12.95 (br, 2H, NH).

$^{31}P\{^1H\}$ NMR data ($^1/_3$benzene-d_6 + $^2/_3CH_2Cl_2$, 19 °C, δ): 36.45 (s, $^1J_{W-P}$ = 140 Hz, $^2J_{P-P}$ = 76.3 Hz).

FAB/DIP MS (NBA, *m/z*): 1038 ($[M]^+$), 1003 ($[M - Cl]^+$), 967 ($[M - 2Cl]^+$), 931 ($[M - 3Cl]^+$).

(iv) *cis,cis*-$W_2Cl_4(NHCMe_3)_2$(dppe) (4). $W_2Cl_4(NHCMe_3)_2(NH_2CMe_3)_2$ (0.5 g, 0.62 mmol) was dissolved in hexanes (10 mL), and dppe (0.25 g, 0.62 mmol) in toluene (10 mL) was transferred by cannula with stirring of the solution. The color of the reaction mixture changed to red, and after about 15 min, a red-brown solid started to precipitate. Stirring was continued for $^1/_2$ h, after which the solid was filtered, washed with hexanes (3 × 5 mL), and dried *in vacuo*. The solid compound was recrystallized at room temperature by slow diffusion of hexanes into a CH_2Cl_2 solution for 1 day to yield orange plates of *cis,cis*-$W_2Cl_4(NHCMe_3)_2$(dppe). A second batch of compound **4** was obtained by cooling the toluene filtrate to 0 °C to give an overall yield of about 39%.

IR data (cm^{-1}): 3157 (m), 3055 (w), 1435 (s), 1365 (m), 1325 (w), 1306 (vw), 1261 (m), 1202 (s), 1173 (vw), 1161 (vw), 1093 (s), 1024 (m), 955 (w), 915 (vw), 864 (m), 816 (ms), 799 (ms), 749 (m), 741 (m), 711 (w), 694 (s), 668 (w).

^1H NMR data (CD_2Cl_2, 24 °C, δ): 1.07 (s, 18H, CMe_3), 2.08 (br, 2H, $P(CH_2)_2P$), 3.63 (br, 2H, $P(CH_2)_2P$), 7.11−7.98 (m, 20H, Ph), 12.76 (br, 2H, NH).

$^{31}P\{^1H\}$ NMR data ($^1/_3$benzene-d_6 + $^2/_3CH_2Cl_2$, 19 °C, δ): 33.85 (s, $^1J_{W-P}$ = 279 Hz, $^3J_{P-P}$ = 21.1 Hz).

FAB/DIP MS (NBA, *m/z*): 1052 ($[M]^+$), 1017 ($[M - Cl]^+$).

Physical Measurements. The IR spectra were recorded on a Perkin-Elmer 16PC FT-IR spectrophotometer as Nujol mulls between KBr plates. ^1H NMR studies (200 MHz) were performed on a Varian XL-200 spectrometer using CD_2Cl_2 or benzene-d_6, and the chemical shifts were referenced to $SiMe_4$ (δ = 0). The $^{31}P\{^1H\}$ NMR data (81 MHz) were obtained at room temperature in 10 mm NMR tubes on a Varian XL-200 broad band spectrometer with the chemical shift values referenced externally and were reported relative to 85% H_3PO_4/D_2O. The FAB/DIP mass spectra were acquired using a VG Analytical 70S high-resolution, double-focusing, sectored (EB) mass spectrometer. The instrument is equipped with a VG 11/250J data system that allowed computer control of the instrument, data recording, and data processing. Samples for analysis were prepared by dissolving neat solid compound in *m*-nitrobenzylalcohol (NBA) matrix on the direct insertion probe tip. The probe was then inserted into the instrument through a vacuum interlock and the sample bombarded with 8 keV xenon primary particles from an Ion Tech FAB gun operating at an emission current of 2 mA. Positive secondary ions were extracted and accelerated to 6 keV and then mass analyzed.

X-ray Crystallographic Procedures. Single crystals of **1**−**4** were obtained as described above in the Experimental Section. Routine unit cell identification and intensity data collection procedures were followed utilizing the options specified in Table 1 and the general procedures previously described.[5] Crystal quality was first checked by means of a rotation photograph. In all cases, lattice dimensions and Laue symmetry were checked using axial photographs. All calculations were performed on a DEC 3000-800 AXP workstation. The coordinates of the tungsten atoms for all of the structures were found in direct-methods *E* maps using the structure solution program in SHELXTL.[6] The

(5) (a) Bino, A.; Cotton, F. A.; Fanwick, P. E. *Inorg. Chem.* **1979**, *18*, 3558. (b) Cotton. F. A.; Frenz, B. A.; Deganello, G.; Shaver, A. *J. Organomet. Chem.* **1973**, 227. (c) Bryan, J. C.; Cotton, F. A.; Daniels, L. M.; Haefner, S. C.; Sattelberger, A. P. *Inorg. Chem.* **1995**, *34*, 1875.
(6) *SHELXTL*, Version 5; Siemens Industrial Automation, Inc., 1994.

Table 2. Selected Bond Distances (Å) and Angles (deg) for *cis,cis*-$W_2Cl_4(NHCMe_3)_2$(dmpm) (**1**), *cis,cis*-$W_2Cl_4(NHCMe_3)_2$(dmpe) (**2**), *cis,cis*-$W_2Cl_4(NHCMe_3)_2$(dppm) (**3**), and *cis,cis*-$W_2Cl_4(NHCMe_3)_2$(dppe) (**4**)

	1	**2**	**3**	**4**
W(1)−W(2)	2.3247(4)	2.3274(5)	2.328(1)	2.3452(5)
W(1)−P(1)	2.508(2)	2.521(2)	2.542(2)	2.555(2)
W(2)−P(2)	2.501(2)	2.528(3)	2.538(2)	2.525(2)
W(1)−N(1)	1.896(6)	1.899(7)	1.895(6)	1.908(7)
W(2)−N(2)	1.911(6)	1.898(7)	1.905(5)	1.912(7)
W(1)−Cl(1)	2.392(2)	2.404(2)	2.381(2)	2.387(2)
W(2)−Cl(4)	2.379(2)	2.390(2)	2.396(2)	2.407(2)
W(1)−Cl(2)	2.445(2)	2.425(2)	2.424(2)	2.410(2)
W(2)−Cl(3)	2.431(2)	2.418(2)	2.400(2)	2.404(3)
P(1)−W(1)−N(1)	95.9(2)	90.9(2)	98.0(2)	98.5(2)
P(1)−W(1)−Cl(1)	160.85(6)	164.03(8)	158.44(6)	159.84(8)
P(1)−W(1)−Cl(2)	77.29(6)	81.15(8)	75.61(5)	76.24(8)
N(1)−W(1)−Cl(1)	98.8(2)	97.1(2)	98.5(2)	95.5(2)
N(1)−W(1)−Cl(2)	140.9(2)	141.2(2)	146.1(2)	140.7(2)
Cl(1)−W(1)−Cl(2)	83.56(6)	84.00(9)	82.94(6)	83.74(9)
W(2)−W(1)−P(1)	89.77(5)	92.54(6)	91.62(4)	94.14(7)
W(2)−W(1)−N(1)	100.7(2)	101.5(2)	99.6(2)	99.8(2)
W(2)−W(1)−Cl(1)	99.52(5)	99.36(6)	99.11(6)	97.73(8)
W(2)−W(1)−Cl(2)	117.55(5)	116.61(6)	113.67(6)	119.31(6)
P(2)−W(2)−N(2)	94.8(2)	91.4(2)	98.5(2)	93.0(2)
P(2)−W(2)−Cl(3)	76.16(7)	79.76(9)	76.86(5)	81.65(7)
P(2)−W(2)−Cl(4)	159.65(7)	162.63(8)	160.73(6)	161.97(8)
N(2)−W(2)−Cl(3)	143.2(2)	142.8(2)	146.5(2)	143.9(2)
N(2)−W(2)−Cl(4)	100.0(2)	97.7(2)	95.2(2)	94.6(2)
Cl(3)−W(2)−Cl(4)	83.64(7)	84.12(9)	84.21(6)	82.55(8)
W(1)−W(2)−P(2)	90.30(5)	93.52(6)	90.51(4)	95.10(5)
W(1)−W(2)−N(2)	99.4(2)	99.6(2)	99.4(2)	100.9(2)
W(1)−W(2)−Cl(3)	115.98(5)	116.80(6)	113.74(6)	115.01(7)
W(1)−W(2)−Cl(4)	100.91(5)	99.52(6)	100.51(5)	99.43(7)

positions of the remaining non-hydrogen atoms were located using subsequent sets of least-squares refinement cycles followed by difference Fourier syntheses employing the SHELXL-93 structure refinement program.[7] These positions were initially refined with isotropic displacement parameters and then with anisotropic displacement parameters to convergence. In each model, hydrogen atoms were introduced in idealized positions for the calculation of structure factors, and the entire model was refined to convergence. Important crystallographic details pertinent to individual compounds are presented in the following paragraphs. Table 2 lists the selected bond distances and angles for each of the structures. Table 3 tabulates the torsional angles along the W≡W bond in each structure. Tables of atomic coordinates and anisotropic displacement parameters as well as complete tables of bond distances and angles and coordinates of hydrogen atoms are available as Supporting Information.

***cis,cis*-$W_2Cl_4(NHCMe_3)_2$(dmpm) (1).** A red block-shaped crystal with the approximate dimensions of 0.45 × 0.35 × 0.30 mm was attached to the end of a quartz fiber with grease and immediately placed in a cold stream of nitrogen (−150 °C). Intensity data were collected on an Enraf-Nonius CAD-4S diffractometer equipped with graphite-monochromated Mo Kα radiation. The unit cell constants were determined from the geometrical parameters of 25 well-centered reflections in the range $21° < 2\theta < 28°$. The unit cell constants and axial photographs were consistent with a monoclinic lattice. Data collection was carried out with an $\omega-2\theta$ scan motion in the range $4° < 2\theta < 50°$. Three standard reflections measured every 1 h revealed negligible decay. Correction for Lorentz, polarization, and absorption effects were applied. The latter correction was based on azimuthal scans of three reflections with the Eulerian angle χ near 90°. The computations were done with Enraf-Nonius SDP software.[8] From the systematic absences in the data, the space group was uniquely determined to be $P2_1/n$. A total of 208 parameters were varied in the final anisotropic refinement for all atoms except hydrogen atoms, to give $R = 0.032$ (for 3763 reflections with $I > 2\sigma(I)$) and $R = 0.039$ (for all 4160 data). The largest peak in the final difference Fourier map was 2.16 e/Å^3, located in the vicinity of the W atoms.

***cis,cis*-$W_2Cl_4(NHCMe_3)_2$(dmpe) (2).** A red rhomboidal crystal with dimensions of 0.25 × 0.18 × 0.13 mm was mounted on the top of a glass fiber with epoxy resin. Diffraction data were collected at 20 °C on a Rigaku AFC5R diffractometer using Cu Kα radiation, and reflections suitable for indexing were found using the automatic search routine. A least-squares analysis of the setting angles of 25 reflections with $46° < 2\theta < 68°$ provided accurate unit cell parameters (Table 1). Three standard reflections were measured during data collection and displayed no systematic variation in intensity. A total of 3897 reflections in the range $7° < 2\theta < 120°$ were collected using the $\omega-2\theta$ scan technique. Empirical absorption corrections based on ψ scans of six reflections were applied to the data set using the TEXSAN software package.[9] The space group was assigned as $P2_1/n$ from the systematic absences in the data. Final least-squares refinement of 225 parameters resulted in $R = 0.034$ (for 3316 reflections with $I > 2\sigma(I)$) and $R = 0.042$ (for all 3722 data). The final difference map was essentially featureless, the largest peaks being associated with the W atoms.

***cis,cis*-$W_2Cl_4(NHCMe_3)_2$(dppm) (3).** A block-shaped red crystal with dimensions of 0.53 × 0.25 × 0.20 mm was mounted on the tip of a quartz fiber with grease and quickly placed in the cold stream at −60 °C of the low temperature controller model FR 558-S. Intensity data were collected on an Enraf-Nonius FAST automated diffractometer with an area detector for $5° < 2\theta < 50°$ using Mo Kα radiation. The general procedures have been fully described elsewhere.[5c] A preliminary data collection was first carried out to afford all parameters and an orientation matrix. Fifty reflections were used in indexing and 250 reflections with $18° < 2\theta < 42°$ in cell refinement. Systematic absences uniquely determined the space group as $P2_1/c$. The data were corrected for Lorentz and polarization effects by the MADNES program.[10] Reflection profiles were fitted, and values of F^2 and $\sigma(F^2)$ for each reflection were obtained by the program PROCOR, which uses a fitting algorithm developed by Kabsch.[11] The reflection data file was reformatted by the program for use with the SHELXL-93 structure refinement software package. The data were corrected for absorption anisotropy effects by an empirical method based on the difference in observed intensities of symmetry and/or azimuth rotation equivalent reflections, and all equivalent reflections merged, using a local adaptation of the program SORTAV.[12] After isotropic refinement of all atoms of the dinuclear complex, the difference Fourier map showed several peaks that could be ascribed to solvent molecules. These peaks were modeled as CH_2Cl_2 solvent molecules, and the crystal contains four dichloromethane molecules in the unit cell. In each CH_2Cl_2 molecule, both Cl atoms were found to be disordered at three positions each. Full refinement of 437 parameters led to residuals of $R = 0.042$ (for 5165 reflections with $I > 2\sigma(I)$) and $R = 0.056$ (for all 6130 data). The final difference Fourier map revealed only one peak above 1 e/Å^3, lying 0.87 Å from W(2).

***cis,cis*-$W_2Cl_4(NHCMe_3)_2$(dppe) (4).** An orange platelike crystal having dimensions of 0.40 × 0.13 × 0.05 mm was coated with grease and mounted on the tip of a quartz fiber. The data collection procedures at −60 °C on an Enraf-Nonius FAST diffractometer using Mo Kα radiation were essentially the same as those for the crystal of **3**. Fifty reflections were employed in cell indexing and 250 reflections in cell refinement. Axial images were used to confirm the Laue group and cell dimensions. No absorption correction was applied. Crystals of **4** conformed to the space group $P2_1/n$ based on the systematic absences in the data. Final anisotropic refinement of 403 parameters resulted in $R = 0.050$ (for 5689 reflections with $I > 2\sigma(I)$) and $R = 0.062$ (for all 6666 data). The final difference map contained several small "ghost"

(7) Sheldrick, G. M. *Crystallographic Computing 6*; Flack, H. D., Parkanyi, L., Simon, K., Eds.; Oxford University Press: Oxford, 1993; p 111.
(8) Structure Determination Package, Enraf-Nonius, Delft, The Netherlands, 1979.
(9) *TEXSAN-TEXRAY*, Structure Analysis Package; Molecular Structure Corp., 1985.
(10) Pflugrath, J.; Messerschmitt, A. *MADNES, Munich Area Detector (New EEC) System*, version EEC 11/9/89; with enhancements by Enraf-Nonius Corp.: Delft, The Netherlands. A description of MADNES appears: Messerschmitt, A.; Pflugrath, J. *J. Appl. Crystallogr.* **1987**, *20*, 306.
(11) (a) Kabsch, W. *J. Appl. Crystallogr.* **1988**, *21*, 67; (b) **1988**, *21*, 916.
(12) Blessing, R. H. *Acta Crystallogr.* **1995**, *A51*, 33.

Table 3. Torsion Angles (deg) about the W−W Axis for *cis,cis*-$W_2Cl_4(NHCMe_3)_2$(dmpm) (**1**), *cis,cis*-$W_2Cl_4(NHCMe_3)_2$(dmpe) (**2**), *cis,cis*-$W_2Cl_4(NHCMe_3)_2$(dppm) (**3**), and *cis,cis*-$W_2Cl_4(NHCMe_3)_2$(dppe) (**4**)

	1	**2**	**3**	**4**
P(1)−W(1)−W(2)−P(2)	46.22(7)	59.93(8)	43.63(5)	56.82(7)
P(1)−W(1)−W(2)−N(2)	141.1(2)	151.9(2)	142.4(2)	150.9(2)
P(1)−W(1)−W(2)−Cl(3)	−28.50(7)	−20.4(1)	−32.22(6)	−26.33(8)
P(1)−W(1)−W(2)−Cl(4)	−116.69(7)	−108.56(9)	−120.47(6)	−112.46(8)
N(1)−W(1)−W(2)−P(2)	142.2(2)	151.3(2)	142.1(2)	156.1(2)
N(1)−W(1)−W(2)−N(2)	−122.9(3)	−116.7(3)	−119.2(2)	−109.8(3)
N(1)−W(1)−W(2)−Cl(3)	67.4(2)	71.0(2)	66.2(2)	73.0(2)
N(1)−W(1)−W(2)−Cl(4)	−20.8(2)	−17.1(2)	−22.0(2)	−13.1(2)
Cl(1)−W(1)−W(2)−P(2)	−116.95(7)	−109.39(8)	−117.60(6)	−106.85(8)
Cl(1)−W(1)−W(2)−N(2)	−22.0(2)	−17.4(2)	−18.9(2)	−12.8(2)
Cl(1)−W(1)−W(2)−Cl(3)	168.32(7)	170.3(1)	166.55(6)	169.99(8)
Cl(1)−W(1)−W(2)−Cl(4)	80.13(7)	82.12(9)	78.31(7)	83.86(9)
Cl(2)−W(1)−W(2)−P(2)	−29.29(7)	−21.45(9)	−31.36(6)	−19.72(8)
Cl(2)−W(1)−W(2)−N(2)	65.6(2)	70.5(2)	67.4(2)	74.4(2)
Cl(2)−W(1)−W(2)−Cl(3)	−104.01(7)	−101.8(1)	−107.21(6)	−102.87(9)
Cl(2)−W(1)−W(2)−Cl(4)	167.80(7)	170.07(9)	164.54(6)	171.00(9)

Scheme 1

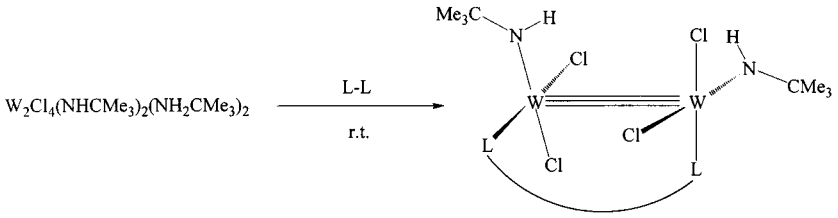

L-L = dmpm, dmpe, dppm, dppe

peaks in close proximity to the heavy atoms, but no effort was made to correct for this problem.

Results and Discussion

Synthesis. All *cis,cis*-$W_2Cl_4(NHCMe_3)_2$(L-L) (L-L = dmpm, dmpe, dppm, dppe) compounds reported herein are formed straightforwardly from the reaction of $W_2Cl_4(NHCMe_3)_2(NH_2CMe_3)_2$ with 1 equiv of the appropriate bidentate phosphine ligands (L-L) at ambient temperature (Scheme 1). These products are obtainable in yields of 39−45%. Compounds **1**−**4** are readily soluble in CH_2Cl_2 and slightly soluble in toluene and benzene. However, they are insoluble in hexanes. In the solid state, all the compounds may be handled in air for short periods of time. In solution, they decompose within 5 min of exposure to air to form brown solutions. We were able to identify one of the decomposition products to be the mononuclear W(IV) species $[WOCl(dmpe)_2]^+$ [13] and $[WOCl(dppe)_2]^+$ [14] for **2** and **4**, respectively, on the basis of $^{31}P\{^1H\}$ NMR and UV spectral data.

Spectroscopic Properties. All the complexes **1**−**4** show absorption bands in the IR spectra above 3000 cm^{-1} due to ν(N−H). The FAB/DIP mass spectra of compounds **1**−**4** all exhibit small molecular ion peaks and comparatively more intense peaks attributable to $[M - Cl]^+$.

Compounds $W_2Cl_4(NHCMe_3)_2$(L-L) show ^1H NMR spectra consistent with the presence of a C_2 symmetry axis and are fully consistent with the solid state structures (*vide infra*). The alkylamide N-protons are evident in the ^1H NMR spectra of **1**−**4** and appear as broad signals in the range 12.21−12.95 ppm. On the other hand, the $^{31}P\{^1H\}$ NMR spectra of all the compounds **1**−**4** consist of strong central singlets flanked by weak satellites due to $^{183}W-^{31}P$ coupling (^{183}W is 14.3% abundant with $S = {}^1/_2$). Table 4 compares the $^{31}P\{^1H\}$ NMR data for the complexes **1**−**4** and their corresponding free ligands. The diphosphine ligands were found to experience significant downfield shifts in the $^{31}P\{^1H\}$ NMR signals upon coordination to the dinuclear W_2^{6+} unit. The largest chemical shift difference is about 65.9 ppm. This reflects the electron-withdrawing capability of the ditungsten units in these complexes. In all cases, only those molecules with one ^{183}W nucleus can cause observable satellites. In addition, the satellites in compounds **1**−**4** are further split into doublets which, for an ABX spin system, $PP^{183}W$, here, will be proportional to J_{A-B} (i.e., J_{P-P}). Clearly, for all the *cis,cis* isomers reported here, the P−P coupling constants are large enough to give a resolved splitting of the satellites. In each case, approximate P−P coupling constants may be obtained from the spectra. For compounds **2** and **4**, the $^1J_{W-P}$ values (305 Hz for **2**, 279 Hz for **4**) are comparable to those reported for *cis*-$W_2Cl_4(NHCMe_3)_2(PR_3)_2$ (R_3 = Me_3, Et_3, Pr^n_3, Me_2Ph).[1b] It is noteworthy that for complexes **1** and **3** containing dmpm and dppm ligands, the $^1J_{W-P}$ values are only 150 and 140 Hz, respectively. However, J_{P-P} values are considerably larger because they are $^2J_{P-P}$ rather than $^3J_{P-P}$ couplings.

Table 4. Comparison of $^{31}P\{^1H\}$ NMR Data for Complexes **1**−**4** and their Corresponding Free Ligands, Measured under Identical Conditions

	δ	$\Delta\delta$, ppm
$W_2Cl_4(NHCMe_3)_2$(dmpm) (**1**)	10.29 (C_6D_6)	65.91
dmpm	−55.62 (C_6D_6)	
$W_2Cl_4(NHCMe_3)_2$(dmpe) (**2**)	13.74 ($CDCl_3$)	60.84
dmpe	−47.10 ($CDCl_3$)	
$W_2Cl_4(NHCMe_3)_2$(dppm) (**3**)	36.45 (C_6D_6/CH_2Cl_2)	59.42
dppm	−22.97 (C_6D_6/CH_2Cl_2)	
$W_2Cl_4(NHCMe_3)_2$(dppe) (**4**)	33.85 (C_6D_6/CH_2Cl_2)	46.76
dppe	−12.91 (C_6D_6/CH_2Cl_2)	

Molecular Structures. Crystal structures of *cis,cis*-$W_2Cl_4(NHCMe_3)_2$(L-L) (L-L = dmpm (**1**), dmpe (**2**), dppm (**3**), dppe (**4**)) are very similar. They all crystallize in the centrosymmetricmonoclinic space group $P2_1/n$ ($P2_1/c$ for **3**·CH_2Cl_2) with four molecules (comprising two pairs of enantiomeric molecules)

(13) Cotton, F. A.; Llusar, R. *Acta Crystallogr.* **1988**, *C44*, 952.
(14) (a) Levason, W.; McAuliffe, C. A.; McCullough, F. P., Jr. *Inorg. Chem.* **1977**, *16*, 2911. (b) Cotton, F. A.; Mandal, S. K. *Eur. J. Solid State Inorg. Chem.* **1991**, *28*, 775.

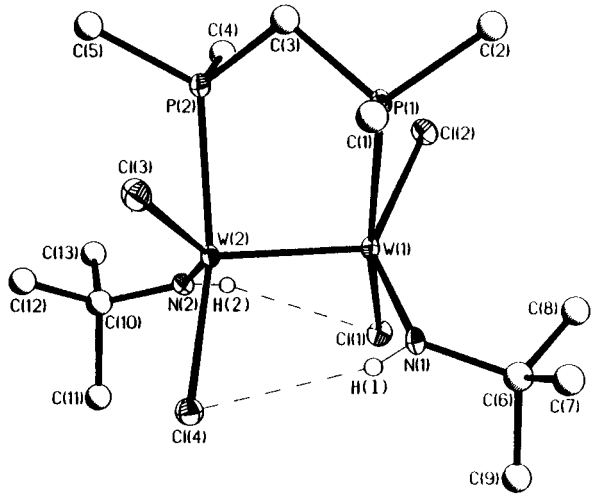

Figure 1. Perspective drawing of *cis,cis*-$W_2Cl_4(NHCMe_3)_2$(dmpm) (**1**). Thermal ellipsoids are shown at the 40% probability level. Carbon atoms are shown as spheres of arbitrary radii. Two hydrogen bonds N-H···Cl are shown as dashed lines.

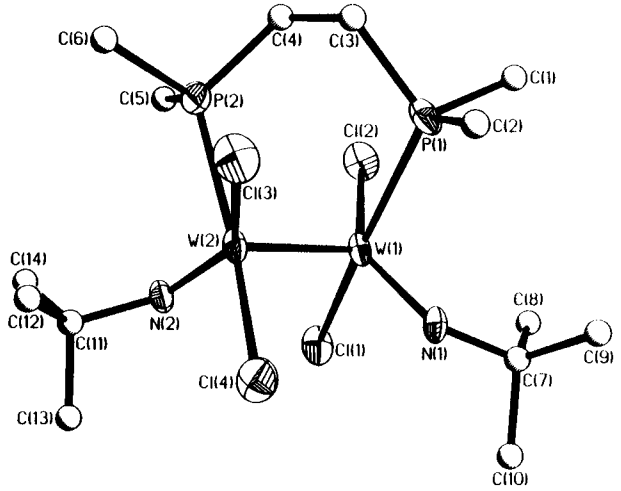

Figure 2. Perspective drawing of *cis,cis*-$W_2Cl_4(NHCMe_3)_2$(dmpe) (**2**). Thermal ellipsoids are shown at the 40% probability level. Carbon atoms are shown as spheres of arbitrary radii.

per unit cell for each complex. Perspective drawings of one molecule of **1**−**4** are depicted in Figures 1−4, respectively. The central portions of each structure consisting of the set of eight ligands are the same, and each has only C_2 symmetry with the 2-fold axis perpendicularly bisecting the W≡W bond. Each molecule is therefore chiral. The W−W bond distances in all of them (**1**, 2.3247(4) Å; **2**, 2.3274(5) Å; **3**, 2.328(1) Å; **4**, 2.3452(5) Å) (Table 2) fall within the range of the bond distances established for the W−W triple bond with a $\sigma^2\pi^4$ configuration.[2] The subtle lengthening in **4** probably reflects steric interaction across the W≡W bond. Each W atom in the molecules is approximately square planar with the two chlorine atoms in a cis arrangement in each WCl_2NP fragment, and the central $(W{\equiv}W)^{6+}$ unit is spanned by a bridging diphosphine. The average W−P bond distances for **1** and **2** (**1**, 2.505(2) Å; **2**, 2.525(3) Å) are shorter than those observed in **3** and **4** (2.540(2) Å in both cases). This difference is presumably due to the increased basicity and smaller size of dmpm and dmpe relative to dppm and dppe. On the other hand, the P−W−N angles are not as large in **3** and **4** as those in **1** and **2** as one would predict from the corresponding ligand sizes. The average W−Cl distances, trans to P, fall in the range 2.386(2)−2.397(2) Å for **1**−**4**, while the mean W−Cl distances, trans to N, are within 2.407(2)−2.438(2) Å (Table 2). These differences in

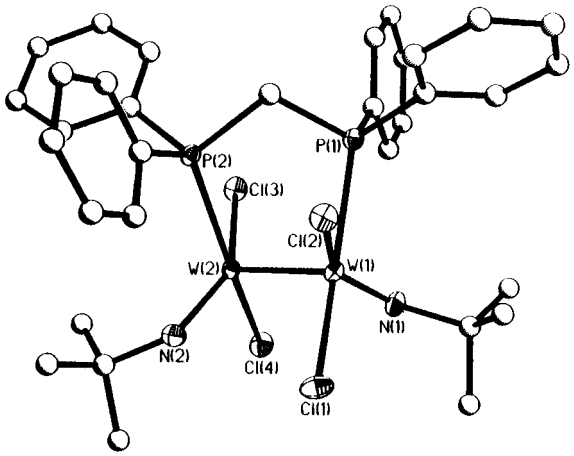

Figure 3. Perspective drawing of *cis,cis*-$W_2Cl_4(NHCMe_3)_2$(dppm) (**3**). Thermal ellipsoids are shown at the 40% probability level. Carbon atoms are shown as spheres of arbitrary radii and are not labeled for clarity.

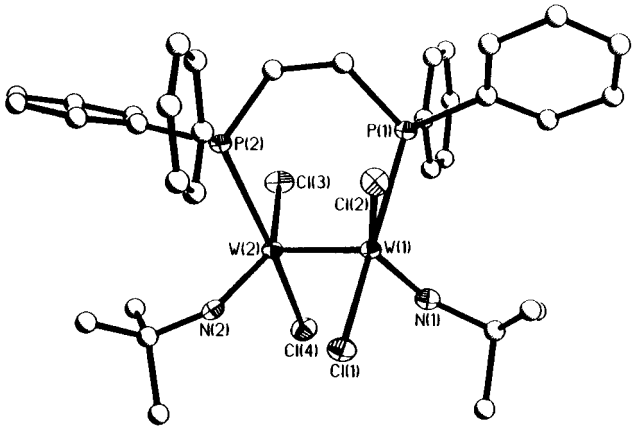

Figure 4. Perspective drawing of *cis,cis*-$W_2Cl_4(NHCMe_3)_2$(dppe) (**4**). Thermal ellipsoids are shown at the 40% probability level. Carbon atoms are shown as spheres of arbitrary radii and are not labeled for clarity.

W−Cl distances are statistically significant, suggesting a stronger structural trans influence of $NHCMe_3$ than that of the phosphine toward the chlorine atoms. The average W−N bond distances of 1.899(7)−1.910(7) Å for all complexes are normal W−NH(R) bond distances of formal bond order 2. One of the most notable features for all the compounds is the twisted configuration of the molecules. Figure 5 illustrates this significant structural aspect for compound **1**, namely that the torsion angle P(1)−W(1)−W(2)−P(2) is exceptionally large (46.2°). The corresponding angle for **3** is 43.6°. However, both **2** and **4** exhibit an even larger conformational twist (Figure 6b) than **1** and **3** (59.9 and 56.8°, respectively), which match well with the longer P−P separation in their structures.

Only two crystal structures of the *cis* isomers of $W_2Cl_4(NHCMe_3)_2(PR_3)_2$ with monodentate phosphines (R_3 = Me_3, Me_2Ph) are known to date.[1a,15] The bond lengths and angles in the central dimetal units of these two complexes are very close to those reported herein for compounds **1**−**4**. In all these *cis* isomers, no disorder of the W_2 units in the crystals was observed, although this was frequently the case for *trans*-$W_2Cl_4(NHCMe_3)_2(PR_3)_2$ (R_3 = Me_3, Et_3, Pr^n_3, Me_2Ph),[1a] which has been addressed to the higher molecular symmetry for *trans* isomers than that for *cis* isomers. The relationship between monodentate phosphine compounds and the title compounds **1**−**4** could be easily

(15) Bradley, D. C.; Hursthouse, M. B.; Powell, H. R. *J. Chem. Soc., Dalton Trans.* **1989**, 1537.

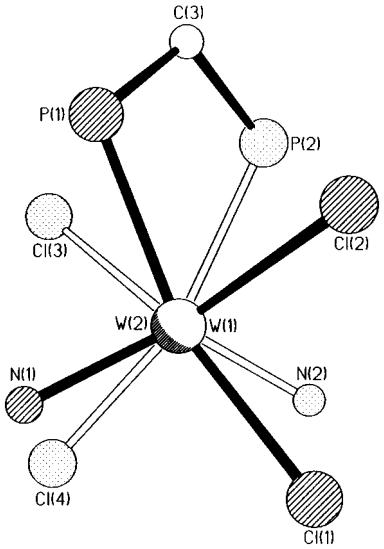

Figure 5. View of the central part of molecule **1** directly down the W(1)−W(2) axis. Methyl and *tert*-butyl groups are omitted for clarity.

visualized in Figure 6, which illustrates the central portion of the molecule down the W≡W axis in each case. It was noted before[1a,4,15] that a very important condition for the stability of $W_2Cl_4(NHCMe_3)_2(PR_3)_2$ complexes is the intramolecular hydrogen bonding N-H···Cl across the W≡W bond with the average Cl−W−W−N torsion angles being 15.5° (PR_3 = PMe_3)[1a] and 15.9° (PR_3 = PMe_2Ph)[15] for the *cis* isomers (Figure 6a). For those two cases, the P−W−W−P angles are 97.3 and 97.8° for PMe_3 and PMe_2Ph, respectively, while these angles are getting smaller in the diphosphine compounds (Figure 6b), leading to a "rotation" of the whole set of ligands (P(2), Cl(3), Cl(4), and N(2)) as compared to the monophosphine counterpart shown in Figure 6a. But the average magnitudes of all corresponding torsion angles for the hydrogen-bonded Cl and N atoms across the W−W vector (−21.4(1), −17.3(2), −20.5(3), −13.0(4)°) still allow the mean N−H···Cl distances to remain within the normal range 2.45−2.58 Å.

Concluding Remarks

Molecules of the general type $W_2Cl_4(NHCMe_3)_2$(L-L), where L-L is a diphosphine, are easily accessible by the reaction of $W_2Cl_4(NHCMe_3)_2(NH_2CMe_3)_2$ with a stoichiometric amount of L-L. The successful isolation of the dppm and dppe derivatives, viz., $W_2Cl_4(NHCMe_3)_2$(dppm) (**3**) and $W_2Cl_4(NHCMe_3)_2$(dppe) (**4**), is particularly interesting since according to an earlier report it was not possible to prepare the triphenylphosphine or (diphenylphosphino)ethane substitution products in this way.[15] These results attest to the stability of the diphosphine as a bridging ligand in the formation of complexes having the stoichiometry $W_2Cl_4(NHCMe_3)_2$(L-L), regardless of the steric bulk of the phenyl groups.

It must be noted that in all four systems studied here, only the *cis,cis* isomer of $W_2Cl_4(NHCMe_3)_2$(L-L) was obtained from *trans,trans*-$W_2Cl_4(NHCMe_3)_2(NH_2CMe_3)_2$, which is presumably the thermodynamically stable product. *In situ* $^{31}P\{^1H\}$ NMR studies of the reaction mixture at the beginning of the experiment suggest that substitution reactions probably take place one by one at each W atom, and we believe that the key initial step in Scheme 1 involves the coordination of one PR_2 group of the diphosphine to one W atom, leaving the other PR_2 moiety free. However, no definite proof is yet available. As time passes, the $^{31}P\{^1H\}$ NMR spectra become complex and additional peaks (including those arising from the *cis,cis* isomer) appear, due presumably to exchange or dissociation processes. There is still much that is not clear about the kinetic and thermodynamic aspects of these reactions. Work relating to this is currently under way.

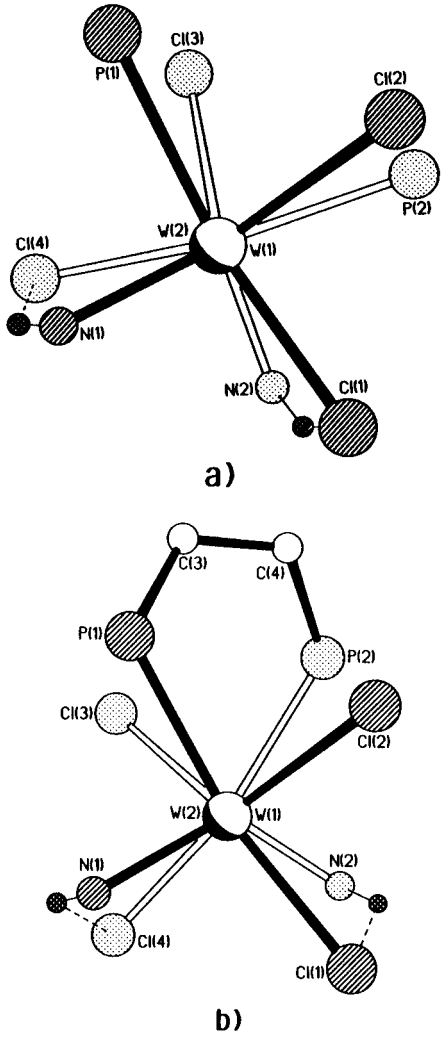

Figure 6. Comparison of the central portions of *cis*-$W_2Cl_4(NHCMe_3)_2(PMe_3)_2$ (a) and molecule **2** (b) directly down the W(1)-W(2) axis. Methyl and *tert*-butyl groups are omitted for clarity. Hydrogen bonding is shown as dashed lines.

Acknowledgment. We thank the National Science Foundation for support.

Supporting Information Available: Four X-ray crystallographic files, in CIF format, are available. Access information is given on any current masthead page.

IC960906Z